

GABA_A presynaptic inhibition regulates the gain and kinetics of retinal output neurons

Jenna Nagy^{1,2,3}, Briana Ebbinghaus^{2,4,5}, Mrinalini Hoon^{1,2,4}, Raunak Sinha^{1,2,4*}

¹Department of Neuroscience, University of Wisconsin, Madison, United States; ²McPherson Eye Research Institute, University of Wisconsin, Madison, United States; ³Cellular and Molecular Pathology Training Program, University of Wisconsin, Madison, United States; ⁴Department of Ophthalmology and Visual Sciences, University of Wisconsin, Madison, United States; ⁵Neuroscience Training Program, University of Wisconsin, Madison, United States

Abstract Output signals of neural circuits, including the retina, are shaped by a combination of excitatory and inhibitory signals. Inhibitory signals can act presynaptically on axon terminals to control neurotransmitter release and regulate circuit function. However, it has been difficult to study the role of presynaptic inhibition in most neural circuits due to lack of cell type-specific and receptor type-specific perturbations. In this study, we used a transgenic approach to selectively eliminate GABA_A inhibitory receptors from select types of second-order neurons – bipolar cells – in mouse retina and examined how this affects the light response properties of the well-characterized ON alpha ganglion cell retinal circuit. Selective loss of GABA_A receptor-mediated presynaptic inhibition causes an enhanced sensitivity and slower kinetics of light-evoked responses from ON alpha ganglion cells thus highlighting the role of presynaptic inhibition in gain control and temporal filtering of sensory signals in a key neural circuit in the mammalian retina.

*For correspondence: raunak.sinha@wisc.edu

Competing interests: The authors declare that no competing interests exist.

Funding: See page 17

Received: 13 July 2020

Accepted: 06 April 2021

Published: 27 April 2021

Reviewing editor: Marla B Feller, University of California, Berkeley, United States

© Copyright Nagy et al. This article is distributed under the terms of the [Creative Commons Attribution License](https://creativecommons.org/licenses/by/4.0/), which permits unrestricted use and redistribution provided that the original author and source are credited.

Introduction

A common motif by which inhibition acts in neural circuits is at the axon terminals of presynaptic neurons where it regulates synaptic release and controls the input-output relationship of a neural circuit (Fink et al., 2014; MacDermott et al., 1999). This motif of inhibition called presynaptic inhibition is widely used in the retina and is mediated by inhibitory retinal interneurons called amacrine cells (ACs) (Diamond and Lukasiewicz, 2012; Eggers and Lukasiewicz, 2011; Eggers et al., 2007; Jadzinsky and Baccus, 2013). ACs make synaptic contacts on the axon terminals of glutamatergic second-order neurons called bipolar cells (BCs) which relay rod and cone photoreceptor signals to retinal output neurons called retinal ganglion cells (RGCs) (Demb and Singer, 2015). Axon terminals of 'ON' BCs – that depolarize in response to a light increment – and 'OFF' BCs – that hyperpolarize in response to a light increment – each stratify at different retinal laminae (Demb and Singer, 2015; Hoon et al., 2014). Of note, different BC types are also used to route dim light (rod bipolar; ON type) and day light (cone bipolar; ON and OFF types) visual signals (Euler et al., 2014). In this study, we explored the role of retinal presynaptic inhibition in regulating the output of one of the most well-characterized retinal circuits that use the ON sustained alpha GC (ON α GC) (Grimes et al., 2014b; Murphy and Rieke, 2006; Schwartz et al., 2012; van Wyk et al., 2009). ON α GCs depolarize and respond with an increase in action potential firing to light increments (Grimes et al., 2014b; Murphy and Rieke, 2006; van Wyk et al., 2009). This ON α GC pathway is not only the most sensitive dim light retinal pathway (Smeds et al., 2019): rod photoreceptors -> rod bipolar cells (RBCs) -> All amacrine -> ON cone bipolar cell (CBC) -> ON α GC; but also one that routes visual signals

directly from cone photoreceptors via ON CBCs for mediating day light vision (*Demb and Singer, 2015; Grimes et al., 2014b; Schmidt et al., 2014; Figure 1A*).

Previous studies have extensively characterized the molecular composition and expression of GABA/Glycine receptors mediating presynaptic inhibition at axon terminals of ON and OFF BCs (*Eggers and Lukasiewicz, 2006; Fletcher et al., 1998; Hoon et al., 2014; Hoon et al., 2015; Lukasiewicz et al., 2004; Matthews et al., 1994; Wässle et al., 1998*). RBCs and ON CBCs predominantly express GABA_A and GABA_C receptors at their axon terminals, whereas OFF CBCs predominantly express GABA_A and glycine receptors (GlyR) at their axon terminals (*Eggers and Lukasiewicz, 2006; Fletcher et al., 1998; Hoon et al., 2015; Lukasiewicz et al., 2004; Wässle et al., 1998*). In the primary rod (dim-light) pathway, presynaptic inhibition has been particularly well characterized where a specialized AC type, the A17 AC, makes GABAergic feedback synapses on RBC axon terminals (*Grimes et al., 2014a; Grimes et al., 2010; Grimes et al., 2015*). This A17-mediated feedback inhibition has been proposed to improve the signal-to-noise ratio of the feedforward excitatory output from RBC to All amacrine cell near visual threshold, extend the luminance range over which RBC-All synapses compute contrast gain, and mediate center-surround inhibition (*Grimes et al., 2015; Oesch and Diamond, 2019; Völgyi et al., 2002*). In addition, a few studies have shown that perturbing GABA_C receptor-mediated presynaptic inhibition alters the dynamic range of the light-evoked responses of RGCs for both rod and cone-mediated signaling (*Oesch and Diamond, 2019; Pan et al., 2016; Sagdullaev et al., 2006*).

Our understanding of how presynaptic inhibition shapes signaling at the BC output synapse largely comes from pharmacological manipulations or transgenic mutant mice globally lacking inhibitory receptor types (*Eggers and Lukasiewicz, 2006; Eggers and Lukasiewicz, 2011; Oesch and Diamond, 2019; Pan et al., 2016; Sagdullaev et al., 2006*). These approaches affect the entire retinal circuitry and thus lack the resolution required to perturb presynaptic inhibition in a cell type-specific and circuit-specific manner. In addition, such methods make it difficult to parse out the role of GABA_A receptor-mediated presynaptic inhibition because, besides BCs, GABA_A receptors are also expressed on ACs that can participate in serial inhibitory circuits between ACs that in turn contact BC terminals (*Eggers and Lukasiewicz, 2011; Wässle et al., 1998*). In fact, immunolabeling against the dominant subunit of GABA_A receptors shows a dense expression, not specific to a single cell class but localized throughout the retinal synaptic layer that makes it particularly difficult to determine the specific contribution of GABA_A receptors in shaping the synaptic output of individual retinal cell types (*Hoon et al., 2015; Wässle et al., 1998; Figure 1B*). Due to these limitations, most studies investigating the role of GABAergic presynaptic inhibition in shaping the light sensitivity of ON BC synapses have largely been restricted to evaluating GABA_C receptor-mediated inhibition that is specifically localized to BCs (*Oesch and Diamond, 2019; Pan et al., 2016; Sagdullaev et al., 2006*). This motivated us to use genetic manipulations that selectively eliminate GABA_A receptors from ON BC axon terminals to study the role of GABA_A receptor-mediated presynaptic inhibition in regulating light evoked function in the tractable retinal circuit of the ON α GC with known cell types and a well-established pathway for dim light and day light signals.

Results

Selective removal of GABA_A receptors from the axon terminals of rod and ON CBCs

In this study, we focused on GABA_A receptor-mediated inhibition at axon terminals of ON BCs. GABA_A receptors expressed in the axon terminals of ON BCs contain $\alpha 1$ and $\gamma 2$ subunits (*Hoon et al., 2015*). To specifically eliminate GABA_A receptors from ON BCs we used a *Gabrg2* (GABA_A receptor, subunit gamma 2) floxed mutant mice (*Schweizer et al., 2003*) crossed to an ON BC specific Cre line (*Grm6-Cre*) and a fluorescent reporter line (*Ai9/tdTomato*) (*Hoon et al., 2015*). This triple transgenic mouse line – *Ai9/Grm6Cre/Gabrg2* cKO (henceforth referred to as KO) – has previously been used to study the subunit composition of GABA_A receptors in axon and dendrites of ON CBCs after *Gabrg2* deletion (*Hoon et al., 2015*). Here we determined the GABA_A and GABA_C receptor expression across axon terminals of RBCs which belong to the ON BC class after *Gabrg2* deletion (*Figure 1B–D*). Immunolabeling with GABA_A $\alpha 1$ receptor subunit specific antibody clearly showed the selective reduction in GABA_A $\alpha 1$ expression from the ON sub-lamina of the inner

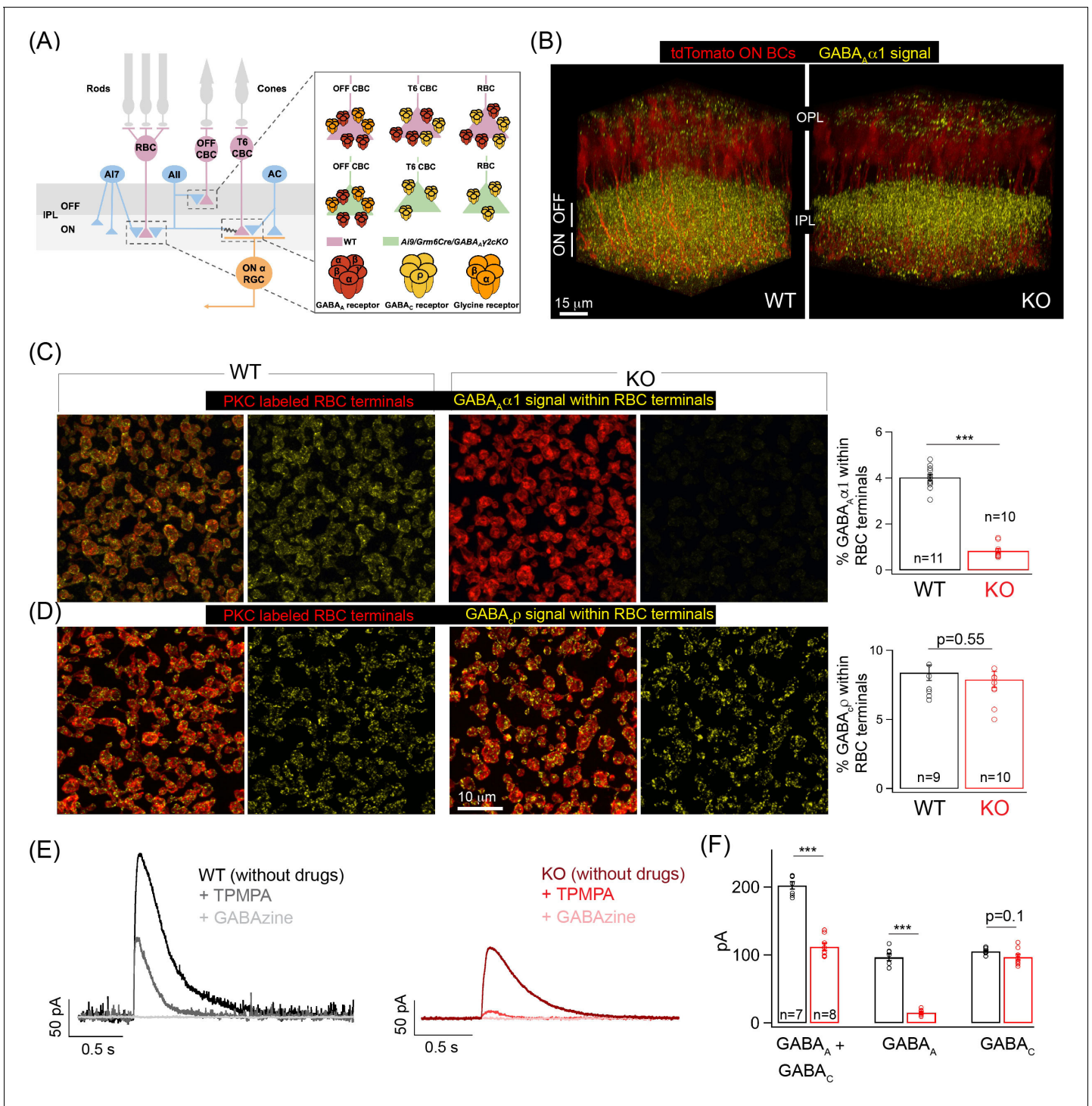


Figure 1. Specific elimination of GABA_A receptors from ON bipolar cell (BC) terminals in the Ai9/Grm6Cre/Gabrg2 conditional knockout (KO) mouse. (A) Schematic illustrating the receptor composition of presynaptic inhibition across rod (RBC) and cone bipolar cell (CBC) axon terminals in wildtype adult littermate control (WT) and KO retina; T6 CBC refers to Type 6 ON CBC (B) $\alpha 1$ -subunit-containing GABA_A receptor (GABA_A $\alpha 1$) immunolabeling (yellow) and ON BC labeling (tdTomato; red) in outer and inner plexiform layers (OPL and IPL respectively) of WT retina and Ai9/Grm6Cre/Gabrg2 (KO) retina. In the KO, GABA_A $\alpha 1$ immunofluorescence is present in the OFF lamina of the IPL but not in the ON lamina. (C) (Left) Immunolabeling of RBC terminals (PKC; red) in WT retina with antibodies against protein kinase C (PKC; red) and GABA_A $\alpha 1$ receptor (yellow; signal within terminals) and protein kinase C (PKC; red) immunolabeling of RBC terminals in WT retina. The merged panel consists of the PKC signal and the receptor signal within PKC positive RBC terminals. (Right) Image of KO retina shows reduced GABA_A $\alpha 1$ receptor immunofluorescence within RBC terminals. (Far right) Quantifications of receptor expression confirmed a significant reduction of GABA_A $\alpha 1$ expression in the KO (mean \pm sem = 0.8 ± 0.1) retina relative to WT (mean \pm sem = 4 ± 0.1). (D) (Left) Immunolabeling of RBC terminals (PKC; red) in WT retina with antibodies against PKC (red) and GABA_B receptor (yellow). The merged panel consists of the PKC signal and the receptor signal within PKC positive RBC terminals. (Right) Image of KO retina shows reduced GABA_B receptor immunofluorescence within RBC terminals. (Far right) Quantifications of receptor expression confirmed no significant change in GABA_B receptor expression in the KO (mean \pm sem = 7.5 ± 0.5) retina relative to WT (mean \pm sem = 8.5 ± 0.5). (E) Electrophysiological traces showing current responses to TPMPA and GABAzine in WT and KO RBCs. (F) Summary bar graph of current amplitudes for GABA_A, GABA_C, and GABA_A + GABA_C responses.

Figure 1 continued on next page

Figure 1 continued

against the ρ -subunit-containing GABA_C receptor (GABA_C ρ ; yellow – signal within RBC terminals). (Right) Image shows GABA_C ρ immunoreactivity within RBC terminals in the KO retina. (Far right) Quantification of RBC terminal GABA_C ρ receptor expression in KO (mean \pm sem = 7.9 ± 0.6) retina relative to WT (mean \pm sem = 8.4 ± 0.6). (E) Exemplar traces of evoked responses of an RBC after GABA puff application at its axon terminal. WT (Left, black trace); KO (Right, red traces). TPMPA (GABA_C receptor antagonist) and GABA_A (GABA_A receptor antagonist) were used to pharmacologically isolate GABA_A and GABA_C receptor-mediated components of the evoked responses. The GABA_A component is revealed after application of TPMPA (labeled +TPMPA) and is eliminated upon the addition of GABA_A (TPMPA + GABA_A; labeled +GABA_A). Note the reduction of the GABA_A receptor-mediated component in the KO relative to the WT. (F) Bar graph quantifying the GABA_A and GABA_C-mediated component of RBC evoked responses in WT (black) and KO (red) retina. The mean \pm sem peak amplitudes of GABA_A + GABA_C currents were 202.5 ± 5.5 pA in WT retina and 112.3 ± 5.6 pA in KO retina. The mean \pm sem peak amplitudes of GABA_A currents were 96.8 ± 5.2 pA in WT retina and 15.2 ± 1.5 pA in KO retina. The mean \pm sem peak amplitudes of GABA_C currents were 105.8 ± 1.8 pA in WT retina and 97 ± 4.3 pA in KO retina. Note that the significant reduction in the total response (GABA_A + GABA_C) in the KO can be attributed to the reduction in the GABA_A-mediated component. In all figures, error bars indicate sem and 'n' refers to the number of cells analyzed except 1C, 1D, and **Figure 1—figure supplement 1E** occupancy quantifications where 'n' refers to the number of retinas analyzed.

The online version of this article includes the following figure supplement(s) for figure 1:

Figure supplement 1. GABA_A inhibition remains intact in OFF cone bipolar cell (CBC), amacrine cell (AC), and ganglion cell (GC) processes in the knockout (KO) mouse.

plexiform layer (IPL) in the KO mice (**Figure 1B**), whereas the GABA_A α 1 expression in the OFF sublamina remained unperturbed (**Figure 1—figure supplement 1A**). Co-labeling of GABA_A α 1 with the RBC marker, protein kinase C (PKC), revealed near-complete absence of GABA_A α 1 receptor subunit expression from RBC boutons in the KO retina (**Figure 1C**). This dramatic reduction in GABA_A α 1 receptor expression in the KO retina was quantified by estimating the receptor percentage volume occupancy relative to the volume of the RBC axon terminal (see 'Materials and methods'). Despite the loss of GABA_A receptors in KO RBC terminals, GABA_C receptor expression was unchanged in KO RBC terminals (**Figure 1D**; quantifications of percentage GABA_C volume occupancy). We confirmed the loss of GABA_A receptors from KO ON BC axon terminals by measuring GABA-evoked currents from RBCs (**Figure 1E**). Puffing GABA on the axon terminals of RBCs elicited smaller currents in the KO retina. Upon application of a selective GABA_C receptor blocker, TPMPA, we found that this decrease in total GABA-evoked current is due to a drastic reduction of the GABA_A receptor-mediated current with unaltered GABA_C currents in KO RBC terminals (**Figure 1F**). To confirm that GABA_A receptors remain unaltered in the OFF sublamina, we performed whole-cell voltage clamp recordings of light evoked excitatory currents from OFF alpha transient GCs (a measure of the OFF BC output) which showed no differences (**Figure 1—figure supplement 1B**) in amplitude between KO and wildtype adult littermate control (WT) retina. This together with the unperturbed GABA_A α 1 expression in the OFF sub-lamina confirms that GABAergic presynaptic inhibition across OFF BCs is not altered in the KO retina.

To eliminate the possibility of decreased GABA_A receptor expression in AC and GC processes in the KO retina, we next determined expression of GABA_A receptors across AC and GC processes that laminate in the same ON plexus of the retinal IPL as ON BC terminals (**Figure 1—figure supplement 1D–E**). We labeled AC and GC processes by labeling for the calcium binding protein calbindin that is specific to AC and GC processes in the IPL (**Haverkamp and Wässle, 2000**). To label all GABA_A receptors across AC and GC processes we labeled for GABA_A β 2/3 receptor subunits which are ubiquitously expressed across BC, AC, and GC processes in the IPL (**Greferath et al., 1995**). We could not label for specific GABA_A α receptor subunits in AC and GC processes as the composition of the GABA_A α receptor types across different AC and GC processes remains unknown and because our previous work has shown that GABA_A α 1-containing receptors are enriched at BC processes (**Hoon et al., 2015**) but not GC processes (**Sawant et al., 2021**). Upon quantification of the percentage occupancy of GABA_A β 2/3 receptors across ON-laminating AC and GC processes we observed comparable receptor amounts across genotypes (**Figure 1—figure supplement 1E**) confirming that expression of GABA_A receptors is not impacted across AC and GC processes in the KO retina. Together, our findings demonstrate the targeted deletion of GABA_A receptors only from the terminals of ON BCs in the KO retina.

Increased sensitivity of ON α GCs to dim light stimuli in the KO retina

We chose the ON α GC retinal circuit as a means to explore the role of presynaptic inhibition in shaping retinal output across luminance (i) due to its well-characterized glutamatergic excitatory pathway – via RBC and Type 6 (T6) ON CBCs (Grimes et al., 2014b; Schwartz et al., 2012) – and (ii) because previous studies have shown that ON BCs, primarily RBC and T6 CBC, express *Grm6* in the *Grm6-tdTomato* transgenic mice (Hoon et al., 2015; Kerschensteiner et al., 2009) and are thus specifically targeted in our triple transgenic mouse line (*Ai9/Grm6Cre/Gabrg2 cKO*). This means that in the KO retina, the majority of the GABA_A receptors lost from the IPL are from RBC and T6 CBC terminals (Figure 1; and see Hoon et al., 2015), thus providing a unique opportunity to study how GABA_A receptor-mediated presynaptic inhibition alters the function of a specific retinal circuit, i.e. the ON α GC circuit (Figure 1A). We first probed the dim light sensitivity of ON α GC spike output using a full-field light stimulus that mostly activates the rods (Figure 2). The characteristic response of an ON α GC to a light step (0.5 s duration) has two distinct kinetic components – a fast transient phase and steady-state sustained phase – which results in action potential firing throughout the duration of the light stimulus (Figure 2B). Such a biphasic response to a sustained dim light step has previously been observed in the excitatory currents of the All amacrine cell and reflects the intrinsic synaptic properties of the RBC to All amacrine cell ribbon synapse (Oesch and Diamond, 2011, Oesch and Diamond, 2019). Furthermore, the transient component has been attributed to encode contrast whereas the sustained component has been shown to encode the absolute luminance (Oesch and Diamond, 2011; Oesch and Diamond, 2019). In the KO retina, there is a sizeable increase in the spike response of ON α GCs for both its transient and sustained component (Figure 2C and D; see 'Materials and methods' for details). In addition to response amplitude, presynaptic inhibition is known to shape the kinetics of neuronal responses across diverse neural circuits (Isaacson and Scanziani, 2011; Jadzinsky and Baccus, 2013; Ohliger-Frerking et al., 2003). We analyzed the time course of the spike responses of the ON α GCs to the dim light step by estimating the time to peak of the response. There was no significant difference in the kinetics of the ON α GC spike responses between KO and WT retina under dim light conditions (Figure 2E).

To determine if the changes in the spike output are present in the excitatory synaptic inputs to the ON α GCs, we performed whole-cell voltage clamp recordings from the ON α GC and measured the excitatory synaptic current evoked by the above dim light stimuli (Figure 2F). The heightened response to the dim light stimuli is in fact more prominent in the excitatory synaptic currents of ON α GCs in the KO retina with nearly a twofold increase in the amplitude of the response in the KO retinas compared to that in the WT retinas (Figure 2G). Both the sustained and transient response components for the ON α GC are equally affected in the KO retina and hence the ratio of sustained to transient response remained unchanged between the WT and the KO retina for light evoked excitatory synaptic currents as well as for spike output (Figure 2D and H). We next estimated the kinetics of the ON α GC dim light evoked excitatory synaptic currents and found that the time to peak of the current response remained unchanged between the WT and the KO retina similar to that for the spike output (Figure 2I; see Figure 2E). To probe if the response differences in ON α GC between KO and WT retina are present across a broad range of dim light levels, we measured responses to brief light flashes (30 ms duration) of increasing intensity under dim light conditions (Figure 2J–M). Both the ON α GC spike output and the excitatory synaptic currents in the KO retina showed a marked increase over a considerable range of dim light flash intensities (Figure 2K and M). This indicates that light-triggered output from the RBC terminals is increased in absence of GABA_A receptors across a wide range of dim light levels albeit not for the dimmest flashes. Moreover, enhancement of both the transient and sustained component of the ON α GC response to a sustained dim light stimulus indicates that perhaps both contrast and luminance encoding are altered at the dim light levels. Although the amplitude of the dim light evoked responses is perturbed, response kinetics remain unaltered in absence of GABA_A receptor-mediated presynaptic inhibition. These results show that GABA_A receptors at the RBC terminal play a key role in regulating the strength of dim light signals received by the ON α GCs presumably by controlling synaptic release from the RBC terminal. We cannot rule out a contribution of loss of GABA_A receptors at the T6 ON CBC towards altered ON α GC sensitivity at dim light levels since rod-driven signals are routed from the All amacrine via gap junctions to the ON CBC terminals and then onto the ON α GC.

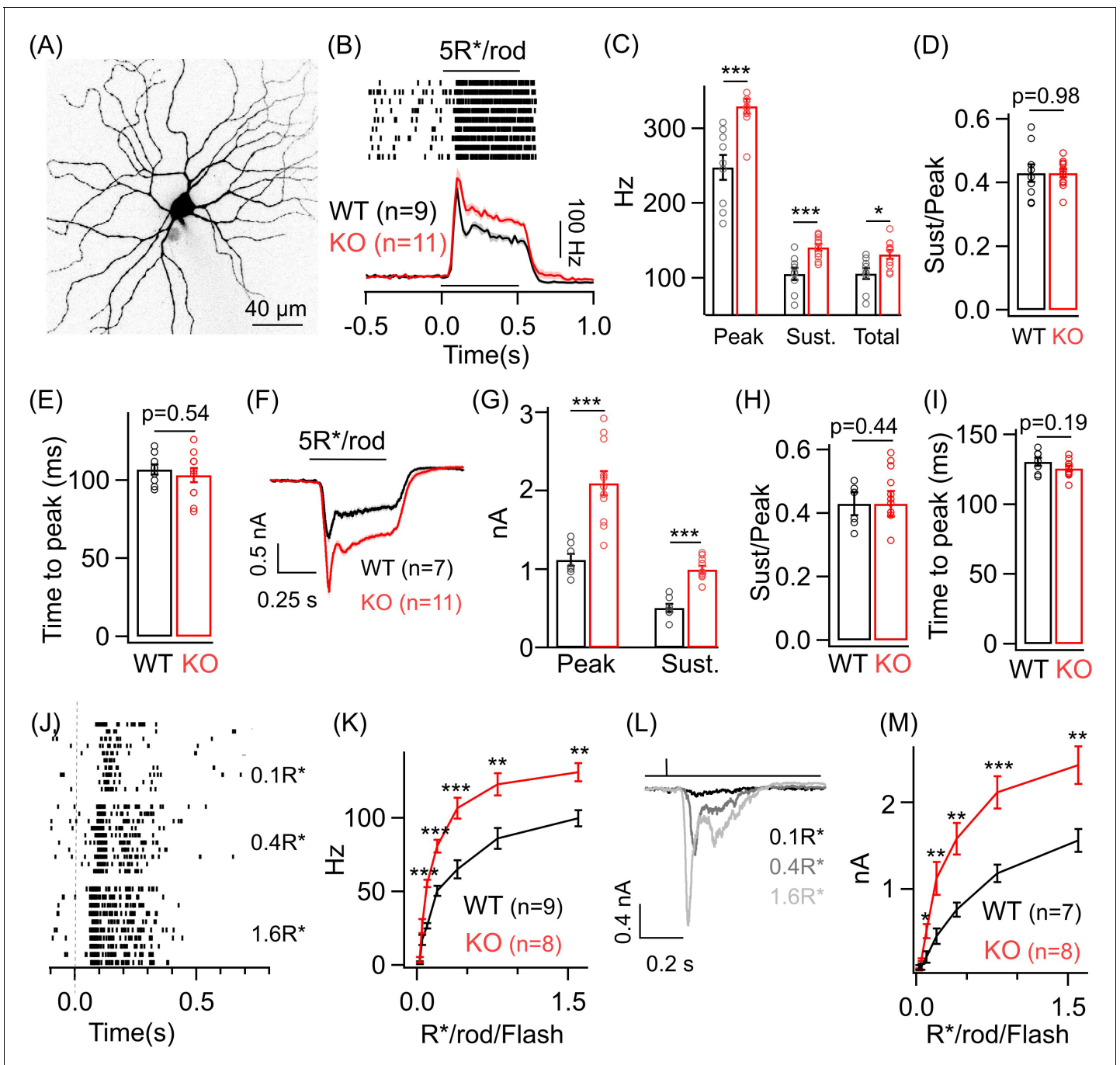


Figure 2. Dim light sensitivity of ON α ganglion cells (GCs) is perturbed without GABA_A presynaptic inhibition. (A) Exemplanar image of an ON α GC filled with dye post-recording. (B) Raster plot showing an ON α GC spike response to a 0.5 s light step (that leads to five opsin photoisomerizations (R*) per rod photoreceptor) from darkness. Bottom panel shows average peri-stimulus time histograms (PSTH; binwidth of 20 ms) of the spike response from several ON α GCs in WT and KO mouse retina. Error bars (sem) shown in shaded colors henceforth for all average traces. The sample size for each experiment henceforth is mentioned next to the average traces and is the same for the following quantification represented in bar plots. (C) Bar plot comparing the peak (mean \pm sem = 247.7 \pm 16.8 Hz in WT and 329.7 \pm 9.7 Hz in KO retina), sustained (mean \pm sem = 105.4 \pm 8.1 Hz in WT and 140.8 \pm 4.4 Hz in KO retina) and total firing rate (mean \pm sem = 105.6 \pm 7.4 Hz in WT and 131.5 \pm 5.7 Hz in KO retina) across ON α GCs as shown in (B) between WT and KO retina. (D) Bar plot comparing the ratio of sustained to peak firing rate of individual ON α GCs in WT (mean \pm sem = 0.43 \pm 0.03) and KO (mean \pm sem = 0.43 \pm 0.01) retina in response to light stimulus shown in (B). (E) Bar graph comparing the time to peak of spike PSTH (with a binwidth of 2 ms) across ON α GCs in WT (mean \pm sem = 106.9 \pm 3.2 ms) and KO (mean \pm sem = 103.3 \pm 4.5 ms) retina for the same data shown in (B). (F) Average excitatory synaptic currents measured across WT and KO ON α GCs elicited by the light stimulus described in (B). (G, H) Bar plot showing the light-evoked peak (mean \pm sem = 1120.5 \pm 78.8 pA in WT and 2096.2 \pm 155.6 pA in KO retina) and sustained responses (mean \pm sem = 505.2 \pm 51.9 pA in WT and 505.2 \pm 51.9 pA in KO retina) across ON α GCs in WT and KO retina. (I) Bar plot comparing the time to peak of spike PSTH (with a binwidth of 2 ms) across ON α GCs in WT (mean \pm sem = 106.9 \pm 3.2 ms) and KO (mean \pm sem = 103.3 \pm 4.5 ms) retina for the same data shown in (B). (J) Raster plot showing an ON α GC spike response to a 0.5 s light step at three different intensities (0.1R*, 0.4R*, 1.6R*). (K) Line graph showing the light-evoked peak (mean \pm sem = 1120.5 \pm 78.8 pA in WT and 2096.2 \pm 155.6 pA in KO retina) and sustained responses (mean \pm sem = 505.2 \pm 51.9 pA in WT and 505.2 \pm 51.9 pA in KO retina) across ON α GCs in WT and KO retina at three different intensities. (L) Average excitatory synaptic currents measured across WT and KO ON α GCs elicited by the light stimulus described in (J). (M) Line graph showing the light-evoked peak (mean \pm sem = 1120.5 \pm 78.8 pA in WT and 2096.2 \pm 155.6 pA in KO retina) and sustained responses (mean \pm sem = 505.2 \pm 51.9 pA in WT and 505.2 \pm 51.9 pA in KO retina) across ON α GCs in WT and KO retina at three different intensities. *Figure 2 continued on next page*

Figure 2 continued

pA in WT and 993.7 ± 45.5 pA in KO retina) and their ratio (mean \pm sem = 0.45 ± 0.04 in WT and 0.49 ± 0.04 in KO retina) analyzed from individual ON α GCs. (I) Bar graph comparing the time to peak of the excitatory current response across ON α GCs in WT (mean \pm sem = 130.5 ± 3 ms) and KO (mean \pm sem = 125.8 ± 1.9 ms) retina for the same data shown in (F). (J) Spike trains from an exemplar ON α GC showing the response to brief (30 ms duration) light flashes that elicit 0.1, 0.4 and 1.6 R*/rod. (K) Peak spike rates of ON α GC in response to increasing flash strengths at dim light levels in WT and KO retinas. (L) Excitatory synaptic currents measured from an exemplar WT ON α GC elicited by light flashes shown in (J). (M) Peak excitatory current response of ON α GCs in response to increasing flash strengths at dim light levels in WT and KO retinas.

ON α GCs in the KO retina exhibit changes in amplitude and kinetics of responses to light stimuli that preferentially excite the cone photoreceptors

Given the increase in dim light sensitivity of ON α GCs in the KO retina, we wanted to test if this persists even for brighter light levels that primarily activate the cone pathway. To do so, we adapted the retina to a background luminance of ~ 1000 R*/cone/s, which mostly saturates the rods (Grimes et al., 2018) and allows us to preferentially probe the cone-mediated ON α GC responses. We first measured the spike response of ON α GCs to a full-field 100% contrast increment (Figure 3A). The ON α GC response at these cone-dominated light levels also shows two kinetic phases, i.e. a transient and sustained phase (Figure 3B), similar to the responses at dim light levels shown in Figure 2. We observed a nearly twofold increase in the peak firing rate of the ON α GC in the KO retina compared to that in the WT retina. However, we did not see a systematic difference in the sustained phase of the spike response of ON α GCs between WT and KO retina (Figure 3—figure supplement 1B). Next, we compared the kinetics of the spike responses of the ON α GCs between KO and WT retina (Figure 3D). Interestingly, the time to peak of the ON α GC spike responses in the KO retina were significantly slower than in the WT retina in contrast to our earlier observations under dim light conditions (Figure 3D). To determine if the changes in the amplitude and kinetics of the cone-mediated spike responses are reflected in the excitatory inputs, we performed whole-cell voltage clamp recordings from ON α GCs in KO and WT retina in response to the above stimuli (Figure 3E). Both the transient and sustained phase of the light-evoked excitatory synaptic current were ~ 2 -fold larger in the KO retina compared to that in the WT retina (Figure 3F). The ratio of the sustained-to-transient phase of the ON α GC response remained unchanged between KO and WT retina (Figure 3G). Upon comparing the response kinetics of ON α GC excitatory currents between KO and WT retina, we observed that the time to peak was higher in the KO retina than in the WT retina similar to the effects on the spike output seen earlier (Figure 3H). We further quantified the time of onset of the sustained phase of the light-evoked excitatory currents in ON α GC but did not observe any significant changes between KO and WT retina (Figure 3—figure supplement 1D,E). The increase in response amplitude and slower time course of the ON α GC excitatory synaptic currents in the KO retina was also evident when we presented a briefer light flash of 10 ms duration (Figure 3I–L). In addition to the longer time taken to reach peak response (Figure 3K), we also found that the decay time of the flash-evoked ON α GC excitatory synaptic currents (from the peak to the baseline) was significantly longer in KO compared to WT retina (Figure 3L). This suggests that GABA_A receptor-mediated presynaptic inhibition regulates both the activation and recovery of the cone-mediated signals at the BC to ON α GC synapse. Given that the size of the flash-evoked ON α GC excitatory currents is ~ 2 -fold larger in KO retina, we wanted to further probe the response recovery, particularly the overshoot after the flash response reaches the baseline (Figure 3M). We estimated the amplitude of the response overshoot from the baseline and observed no difference between ON α GCs in KO and WT retina (Figure 3M).

To ensure that postsynaptic inhibition acting directly on the ON α GC is not significantly perturbed in the KO retina and the differences we see at the level of spike output are due to changes in the excitatory input, we compared light-evoked inhibitory currents from ON α GC to a 100% contrast increment step (Figure 3—figure supplement 2A). There was no change in light-evoked postsynaptic inhibition in ON α GC in the KO retina compared to that in the WT retina indicating that increase in the excitatory inputs most likely cause the increase in the spike output of ON α GC light responses in the KO retina (Figure 3—figure supplement 2B).

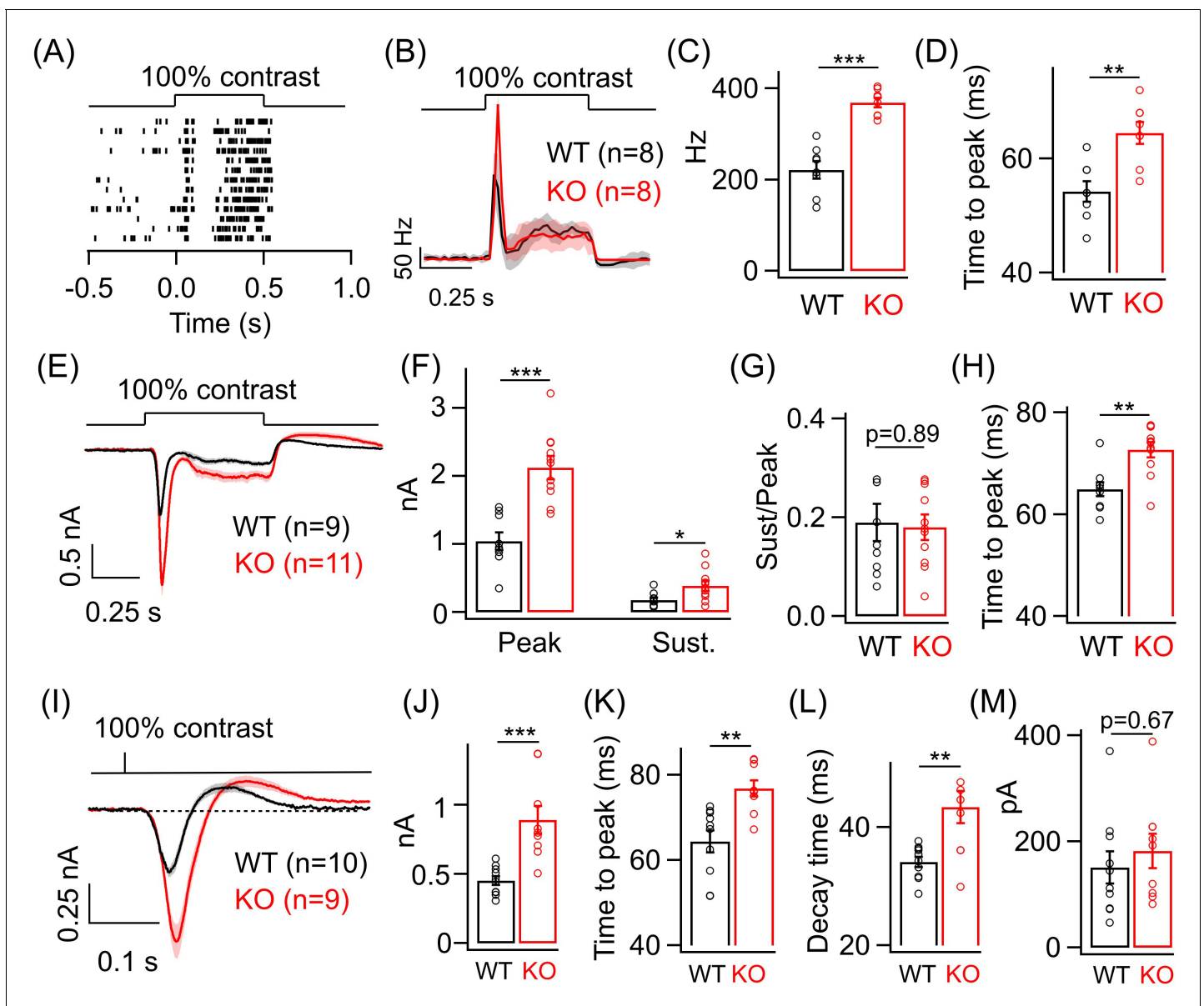


Figure 3. Lack of GABA_A presynaptic inhibition alters ON α ganglion cell (GC) light responses at cone light levels. (A) Exemplar spike raster from an ON α GC in WT retina in response to a 100% contrast step from a background luminance of $\sim 1000R^*/S$ cone/s, where cones dominate retinal responses. (B) Average PSTH (binwidth of 20 ms) of spike response to the light step in A across several ON α GCs with spike rate expressed in Hz (spikes/s). (C) Bar plot showing quantification of the peak firing rates across ON α GCs in WT (mean \pm sem = 221.2 ± 18.9 Hz) and KO retina (mean \pm sem = 368.5 ± 10.2 Hz). (D) Bar graph comparing the time to peak of spike PSTH (with a binwidth of 2 ms) across ON α GCs in WT (mean \pm sem = 54.3 ± 1.8 ms) and KO (mean \pm sem = 64.5 ± 1.9 ms) retina for the same data shown in (B). (E) Average excitatory synaptic current elicited in response to a 100% contrast step across ON α GCs in WT and KO retina. (F) Quantification of peak and sustained current amplitudes in response to the 100% contrast step in E. The mean \pm sem peak amplitudes were 1042.3 ± 127.9 pA in WT retina and 2126 ± 169.5 pA in KO retina. The mean \pm sem amplitudes of the sustained phase were 176.7 ± 36.2 pA in WT retina and 386.9 ± 75.5 pA in KO retina. (G) Quantification of ratio of sustained to peak amplitude in F. The mean \pm sem ratios were 0.19 ± 0.04 in WT retina and 0.18 ± 0.03 in KO retina. (H) Bar graph comparing the time to peak of the excitatory current response across ON α GCs in WT (mean \pm sem = 64.9 ± 1.4 ms) and KO (mean \pm sem = 72.7 ± 1.5 ms) retina for the same data shown in (E-G). (I) Average excitatory synaptic currents in response to 10 ms flash of 100% contrast across ON α GCs in WT and KO retina. (J) Quantification of peak current amplitude in response to the 10 ms flash of 100% contrast step in WT (mean \pm sem = 451.6 ± 32.2 pA) and KO (mean \pm sem = 890.9 ± 100.8 pA) retina as shown in I. (K) Bar graph comparing the time to peak of the excitatory current response across ON α GCs in WT (mean \pm sem = 64.4 ± 2.6 ms) and KO (mean \pm sem = 76.8 ± 1.9 ms) retina for the same data shown in (I). (L) Quantification of decay time of the excitatory current response, i.e. time for the response in (I) to return from the peak to the baseline shown in dotted line, across ON α GCs in WT (mean \pm sem = 34.1 ± 0.9 ms) and KO (mean \pm sem = 43.4 ± 2.8 ms) retina for the same data shown in (I). (M) Quantification of the rebound amplitude

Figure 3 continued on next page

Figure 3 continued

of the excitatory current response across ON α GCs in WT (mean \pm sem = 151 \pm 30.4 pA) and KO (mean \pm sem = 182.4 \pm 32.2 pA) retina for the same data shown in (I).

The online version of this article includes the following figure supplement(s) for figure 3:

Figure supplement 1. Analysis of the sustained phase of the light-evoked spike and excitatory current response in ON α ganglion cells (GCs).

Figure supplement 2. Post-synaptic inhibition remains unchanged in ON α ganglion cell (GC) in the knockout (KO) retina.

These results suggest that loss of GABA_A receptor-mediated presynaptic inhibition alters the amplitude of both rod- and cone-driven signals but only the time course of cone-driven signals received by the ON α GCs.

Temporal sensitivity and contrast encoding of ON α GCs are altered in the KO retina

To compare the temporal filtering and contrast sensitivity of the ON α GCs in WT and KO retina, we used a random time-varying stimulus consisting of a range of temporal frequencies and contrasts (**Figure 4A**; see 'Materials and methods'). To characterize the responses, we used a linear-nonlinear (LN) model that provides a relatively simple description of how light inputs are transformed into neuronal responses and provides an effective way of determining contrast-dependent changes in the amplitude and kinetics of the light response of retinal neurons (**Beaudoin et al., 2007; Kim and Rieke, 2001; Sinha et al., 2017**). The model has two components – a linear filter that describes the time course of the neuronal response and a time-invariant or 'static' nonlinearity that transforms the filtered stimulus into neuronal responses (**Beaudoin et al., 2007; Kim and Rieke, 2001; Rieke, 2001**). We focused on excitatory synaptic currents since the loss of GABA_A receptors at ON BC terminal in the KO retina will directly impact the ON BC output and hence the glutamatergic synaptic input onto the ON α GCs. We measured ON α GC excitatory synaptic currents in response to the time-varying stimuli that were modulated at two background light levels – one that preferentially activate rods and the other that selectively excites the cone photoreceptors (**Figure 4A,H**). At cone light levels, linear filters show that the time course of the ON α GC excitatory current response in the KO retina is considerably slower than in the WT retina (**Figure 4B**). Both the time to peak and the decay time of the linear filters were significantly longer for ON α GC in KO retina compared to WT retina (**Figure 4C**) similar to the above results from the responses to brief light flashes (**Figure 3K,L**). This suggests that lack of GABA_A receptor-mediated presynaptic inhibition alters the temporal filtering of the T₆ CBC output and hence the excitatory inputs in the ON α GCs by likely attenuating higher frequencies more and lower frequencies less. We next compared the static nonlinearity of the ON α GCs in WT and KO retina (**Figure 4E**). We first quantified the response range which we defined as the absolute difference between the maximum and the minimum value of the measured current response to the chosen contrast range (**Figure 4F**). This response range, i.e. dynamic range of the excitatory currents for the given range of contrasts, was ~2-fold larger for the ON α GCs in the KO retina in comparison to their counterparts in the WT retina (**Figure 4F**). This is consistent with our above results of the ON α GC responses to light flash/step of fixed intensity (**Figure 3**). Given the sizeable change in the response amplitude and the response range, we assessed if the contrast gain is altered in the ON α GCs in KO retina compared to that in WT retina. This can be estimated from the slope of the nonlinearity or the height of the linear filter since both the linear filter and the static nonlinearity share contrast-dependent changes in the amplitude of the neuronal response (**Kim and Rieke, 2001; Rieke, 2001**). To unambiguously measure contrast gain, we normalized the linear filter and then compared the slope of the nonlinearity between ON α GC responses in KO and WT retina (see 'Materials and methods'). The nonlinearities of the ON α GC response in KO retina had a steeper slope and upon quantification the slope differed by a factor of ~2 compared to the ON α GC nonlinearities in WT retina (**Figure 4G**). These results suggest that GABA_A presynaptic inhibition tightly regulates contrast sensitivity of the ON α GC excitatory inputs and restricts the response size used for encoding over a range of contrast.

We repeated the above experiments on ON α GCs in WT and KO retina under a dim light background (**Figure 4H–M**). The nonlinearity of the ON α GC in the KO retina also had a bigger response range than in WT retina similar to that observed under cone-driven light levels (**Figure 4K,L**). The

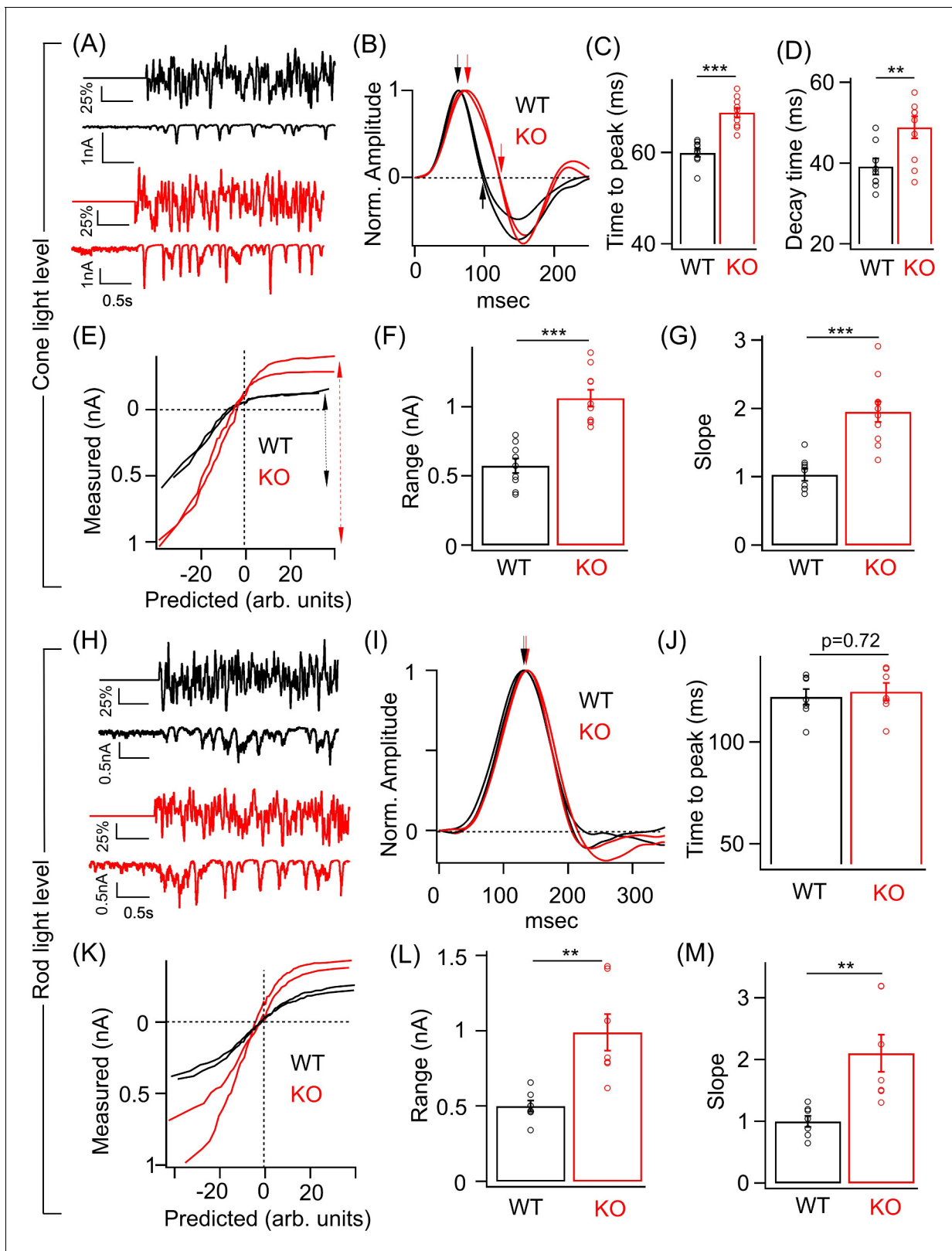


Figure 4. Perturbed ON α ganglion cell (GC) responses to time-varying light stimuli in absence of GABA $_A$ presynaptic inhibition. (A) (Top) Excerpt of the time-varying random white noise stimulus presented at a background luminance of 1000 R*/S cone/s. (Bottom) The resulting excitatory synaptic response used to derive the linear filter and static nonlinearity that relate the stimulus to the response. (B) Exemplar time-reversed linear filters for the responses to noise stimuli for two ON α GCs from WT and KO retina. The black and red arrows point to the time to peak and the time point of decay to

Figure 4 continued on next page

Figure 4 continued

the baseline. Quantification of the time to peak (C) and the decay time (D) in linear filters for responses to stimuli (cone light levels) across ON α GCs in WT (n = 9 cells) and KO (n = 10 cells) retina. The mean \pm sem peak times to peak of the linear filters were 59.9 ± 0.9 ms in WT retina and 68.5 ± 0.9 ms in KO retina. The mean \pm sem decay times of the linear filters were 39.2 ± 2 ms in WT retina and 48.9 ± 2.7 ms in KO retina. (E) Exemplar static nonlinearities of two ON α GCs from KO and WT retina for the noise stimuli. (F) Quantification of the response range (denoted by the dotted black and red arrows) in (E) across ON α GCs in WT (n = 9 cells; mean \pm sem = 573.3 ± 52 pA) and KO (n = 10 cells; mean \pm sem = 1063.5 ± 61.4 pA) retina. (G) Quantification of the nonlinearity slope (see 'Materials and methods') across ON α GCs in WT (n = 9 cells; mean \pm sem = 1 ± 0.1) and KO (n = 10 cells; mean \pm sem = 2 ± 0.2) retina. (H) (Top) Excerpt of the time-varying stimulus presented at a dim background luminance of 10 R*/rod/s. (Bottom) The resulting excitatory synaptic response used to derive the linear filter and static nonlinearity that relate the stimulus to the response. (I) Exemplar time-reversed linear filters for the responses to noise stimuli (under rod light levels) for two ON α GCs from WT and KO retina. The black and red arrows point to the time to peak. (J) Quantification of the time to peak in linear filters for responses to noise stimuli (rod light levels) across ON α GCs in WT (n = 7 cells; mean \pm sem = 122.2 ± 3.9 ms) and KO (n = 7 cells; mean \pm sem = 124.8 ± 4.3 ms) retina. (K) Exemplar static nonlinearities of ON α GC responses for the noise stimuli from WT and KO retina. (L) Quantification of the response range across ON α GCs in WT (n = 7 cells; mean \pm sem = 500.6 ± 37.1 pA) and KO (n = 7 cells; mean \pm sem = 990 ± 121.9 pA) retina. (M) Quantification of the nonlinearity slope (see 'Materials and methods') across ON α GCs in WT (n = 7 cells; mean \pm sem = 1 ± 0.1) and KO (n = 7 cells; mean \pm sem = 2.1 ± 0.3) retina.

slope of the nonlinearity, i.e. contrast gain was also ~ 2 -fold higher for the ON α GC in the KO retina than that in the WT retina (Figure 4M). However, no significant difference in the kinetics of the linear filters between the genotypes was observed (Figure 4J). Our findings of alterations in response size and time course using randomly flickering stimuli are consistent with the results obtained above (Figures 2 and 3) using fixed intensity stimuli. Thus, loss of GABA_A receptor-mediated presynaptic inhibition at the RBC and T6 CBC terminal alters the contrast sensitivity and kinetics of the ON α GC excitatory inputs. Importantly the changes in response amplitude and kinetics observed at the level of ON α GC excitatory inputs in the KO retina are reflected in the spike output which highlights the importance of GABA_A presynaptic inhibition as a mechanism in shaping visual signals being transmitted out of the retina.

Discussion

Presynaptic inhibition is an important mechanism for regulating a neuron's input-output relationship. However, it has been difficult to isolate its precise contribution in most retinal circuits due to lack of receptor type-, cell type-, and circuit-specific perturbations. Here we have taken advantage of a previously used (Hoon et al., 2015) transgenic manipulation in mouse retina that selectively eliminates a specific population of inhibitory receptors – GABA_A receptors – from the axon terminals of defined types of presynaptic neurons – RBC and T6 CBCs – and determined its impact on the light-evoked response properties of one of the well characterized downstream retinal output neuron – the ON α GC. We show that GABA_A receptor-mediated presynaptic inhibition is crucial for regulating the amplitude and contrast sensitivity of both rod and cone-driven signals routed to the ON α GCs. Interestingly, GABA_A presynaptic inhibition shapes the kinetics of only cone-driven signals but not rod-driven signals reaching the ON α GCs. We show that the impact on the gain and kinetics of visual signals as observed in the excitatory synaptic inputs received by the ON α GCs, is propagated to its spike output. Thus, GABA_A presynaptic inhibition is a key mechanism of gain control and temporal filtering for the ON α GC retinal circuit.

GABA_A presynaptic inhibition shapes rod and cone signaling in the ON α GC retinal circuit

Several studies including our current study have shown that GABA_A and GABA_C receptors in ON BC terminals contribute to nearly equal amplitudes of GABA-evoked currents (Hoon et al., 2015; Sinha et al., 2020). However, most of what we know about the role of presynaptic inhibition in shaping the retinal RBC (Pan et al., 2016) and ON CBC synaptic output has been attributed to GABA_C receptor-mediated inhibition (Oesch and Diamond, 2019; Sagdullaev et al., 2006). In the current study, we show that GABA_A receptor-mediated presynaptic inhibition plays an equally important role in regulating the dynamic range and contrast sensitivity as GABA_C receptor-mediated presynaptic inhibition for both the RBC output under dim light conditions as well as for cone-mediated signals via the ON CBC synapse. GABA_A receptor-mediated presynaptic inhibition restricts the response range and contrast gain of ON α GC responses which could allow the ON α GC retinal circuit to

encode over a wider range of contrast and luminance without being saturated. This is a common feature of light adaptation whereby retinal neurons match their neural gain to the prevailing visual inputs such that they can continue to efficiently signal over a broad range of light inputs (*Rieke and Rudd, 2009*). Thus, our results together with previous findings (*Oesch and Diamond, 2019; Sagdullaev et al., 2006*) suggest that both GABA_A and GABA_C presynaptic inhibition play a key role in regulating response amplitude and contrast encoding under rod- and cone-dominant lighting conditions.

A central role of presynaptic inhibition that has not been extensively explored in the retina is how it shapes the temporal sensitivity of rod- and cone-driven signals routed via specific neural circuits (*Asari and Meister, 2012*). Temporal processing is crucial to encode dynamic features of visual signals such as motion (*Jadzinsky and Baccus, 2013*). Temporal filtering, i.e. sensitivity to certain temporal patterns, is different across RGC types, and synaptic inhibition is a common mechanism that is known to shape temporal filtering in most neural circuits (*Baden et al., 2016*). Presynaptic inhibition is well positioned to decrease synapse output and attenuate steady inputs thus temporally filtering signals received by RGCs. Signals originating in rod vs. cone photoreceptors are known to exhibit remarkably distinct temporal characteristics with rod signals being substantially slower compared to cone signals (*Cangiano et al., 2012; Ingram et al., 2016*). This difference is reflected in our results from both fixed intensity and randomly modulating stimuli where the time course of rod signals was nearly 2-fold slower than the cone-mediated signals in WT retina measured at the level of ON α GCs (*Figure 2E and I vs. Figure 3D,H and K; Figure 4C vs J*). Our findings show that GABA_A presynaptic inhibition speeds up the time course of cone-mediated signals but not rod-driven signals in the ON α GC retinal circuit. This could be because under dim light conditions where photons are sparse, a longer integration time of the rod signals by the downstream circuit may benefit signal detection (*Field et al., 2005*). In this case, temporal filtering by mechanisms such as presynaptic inhibition could be detrimental to the detection of sparse signals such as single photons. In fact, recent studies have shown that ON α GCs are one of the most sensitive GC types in the mouse retina under dim light conditions and comprise the major conduit for relaying single photon signals out of the retina (*Smeds et al., 2019*). Hence, minimizing temporal filtering by GABA_A presynaptic inhibition may help prolong the duration of signal integration and may improve sensitivity of the ON α GCs for single photon signaling in near complete darkness.

Besides signaling efficiently at absolute threshold in darkness, the ON α GC retinal circuit also integrates cone-driven signals and can operate under high luminance conditions (*Grimes et al., 2014b; Schwartz et al., 2012; Sonoda et al., 2018*). Our results show that GABA_A presynaptic inhibition limits the response size and contrast gain while speeding up cone-driven signals reaching the ON α GCs. This can have two potential advantages. First, encoding contrast with a smaller response amplitude might allow to effectively signal over a broader dynamic range of contrasts without being saturated. As the contrast range explored in our experiments represent a small fraction of the contrast distribution present in natural scenes, such a gain control mechanism would help match the contrast sensitivity of the ON α GC retinal circuit to the statistics of the prevailing light inputs. Second, being able to signal fast changes in light inputs might aid the ON α GC retinal circuit in the efficient encoding of dynamic features such as during motion.

Our findings that GABA_A presynaptic inhibition regulates the gain and kinetics of visual signals in the ON α GC retinal circuit is consistent with previous studies in other neural circuits, besides the retina, where presynaptic inhibition has been shown to play a central role in gain control and temporal filtering of neural signals (*Baden and Hedwig, 2010; Chen and Regehr, 2003; Fink et al., 2014; Frerking and Ohliger-Frerking, 2006*). For instance, presynaptic inhibition mediated by GABAergic interneurons contributes to motor behavior in the spinal cord, where it controls the gain of sensory afferents and mediates smooth muscle movement (*Fink et al., 2014*). In the olfactory system, GABAergic presynaptic inhibition of the olfactory sensory axon terminals serves as a primary gain control mechanism to maintain odor sensitivity over a wide range of inputs (*Olsen and Wilson, 2008; Root et al., 2008*). Additionally, presynaptic inhibition mediated by GABA receptors controls temporal contrast enhancement and modifies odor-guided navigation in *Drosophila melanogaster* (*Raccuglia et al., 2016*).

Presynaptic inhibition regulates neurotransmitter release and synapse arrangement

The role of presynaptic inhibition is particularly important for the ON α GC pathway. Previous studies have shown that excitatory synaptic inputs dictate the spike output of the ON α GCs (*Murphy and Rieke, 2006*), and we show that GABA_A presynaptic inhibition is a key mechanism well-poised to shape the ON α GC excitatory synaptic inputs. Both GABA_A and GABA_C receptors are localized at axon terminals of ON BCs, but they have been shown to be present at spatially distinct sites at RBC terminals relative to the site of synaptic release, i.e. ribbon (*Grimes et al., 2015*). Pharmacological blockade and genetic deletion of GABA_C receptors have shown that GABA_C receptor-mediated presynaptic inhibition regulates the extent of multivesicular glutamate release at the bipolar ribbon-type synapses (*Oesch and Diamond, 2019; Sagdullaev et al., 2006*). Particularly in the ON CBC synapse, loss of GABA_C receptors results in activation of the perisynaptic NMDA receptors on RGC dendrites by glutamate spillover from the synapse thus enhancing synaptic output (*Sagdullaev et al., 2006*). This could be a potential underlying mechanism for the enhanced light-evoked response we observe in ON α GCs in absence of GABA_A receptors on the ON CBC terminals.

In RBCs, luminance and contrast are encoded via dynamic release and replenishment of the readily releasable pool (RRP) of synaptic vesicles located at the ribbon (*Oesch and Diamond, 2011; Oesch and Diamond, 2019*). A step increase in luminance results in contrast encoding via a transient bout of vesicle release from the RRP, which corresponds to a transient peak in the All AC excitatory current. The size of the remaining vesicle pool is used to encode luminance and corresponds to the sustained component of the excitatory postsynaptic current. A17 AC-mediated feedback inhibition on RBCs acting via GABA_C receptors has been implicated in regulating the extent of RRP depletion and synaptic output from RBCs which in turn shapes luminance and contrast encoding across a range of dim light levels (*Oesch and Diamond, 2019*). Our results show that lack of GABA_A receptors in the RBC and T6 CBC terminals affects both the transient and sustained components of RBC and T6 CBC output as measured from the impact on the ON α GC excitatory inputs under rod- and cone-dominant light conditions. This indicates that both contrast and luminance encoding in the RBC and T6 CBC pathway might be shaped by GABA_A receptor-mediated presynaptic inhibition. However, we cannot distinguish between the contribution of 'feedback' vs. 'lateral' GABA_A receptor-mediated presynaptic inhibition at RBC and T6 CBC terminal on ON α GC function. Feedback presynaptic inhibition on BC terminals is mediated by an AC that is activated by the same BC it provides inhibition onto, and lateral presynaptic inhibition is mediated by ACs activated by other BCs (*Asari and Meister, 2012; Grimes et al., 2015*).

It is well established that for most synapses the input-output relationship of membrane voltage vs. transmitter release is nonlinear and has a sigmoidal shape (*Neher and Sakaba, 2008*). Previous studies have in fact proposed that this synaptic transfer function of the ON CBC terminals has a sigmoidal relationship between membrane voltage and glutamate release with a steep nonlinear foot (*Grimes et al., 2014b*). The ON CBC or presynaptic membrane potential can be influenced by gap junctional coupling from the All amacrine cell processes which can alter synapse output by changing its location on the voltage-release curve. This form of regulating synaptic output has been shown to play a critical role in shaping ON α GC function (*Grimes et al., 2014b*). GABA_A receptor-mediated presynaptic inhibition could also regulate the presynaptic membrane voltage of the ON CBC, thereby controlling the set point of the synapse input-output curve and hence the ON α GC excitatory inputs.

ON BC synapses are specialized ribbon synapses that often have defined postsynaptic partners. One such example is the RBC output synapse onto All and A17 AC processes (*Grimes et al., 2015*). Our recent study showed that presynaptic inhibition plays a key role in the precise assembly of the ribbon synapse at the RBC terminal and organization with correct postsynaptic partners (*Sinha et al., 2020*). Interestingly, under conditions where expression of both GABA_A and GABA_C receptors in the RBC terminals are downregulated, such as during lack of global inhibitory transmitter release or loss of specific synaptic adhesion molecules, ultrastructural analysis revealed that the RBC ribbon synapse is misorganised and makes erroneous connections with postsynaptic partners (*Sinha et al., 2020*). Therefore, despite the downregulation of both GABA_A and GABA_C receptors at the RBC terminal in this situation, there is decreased dim light sensitivity of the ON α GC output

(Sinha *et al.*, 2020) probably due to a reduced feedforward excitatory drive as a result of synaptic mis-arrangements at the RBC terminal. In the KO mice used in the current study, there is a drastic reduction of GABA_A receptor expression but unaltered GABA_C receptor expression in the RBC terminals. Given that dim light sensitivity is increased in the KO retina, it will be interesting in the future to use ultrastructural techniques in the KO retina to determine if the selective reduction of GABA_A receptors results in any organizational deficits of RBC output (ribbon) synapse assembly.

In conclusion, our study provides the first characterization of how selective perturbation of GABA_A receptor-mediated inhibition at ON BC terminals impacts visual signaling of a well-characterized GC circuit. Future studies will be needed to explore how presynaptic inhibition regulates functional properties of other ganglion cell pathways as well as its contribution to shaping the receptive field organization of ganglion cell types.

Materials and methods

Key resources table

Reagent type (species) or resource	Designation	Source or reference	Identifiers	Additional information
Genetic reagent (<i>Mus musculus</i>)	<i>Gabrg2</i>	Jackson Laboratory	JAX Stock# 016830 RRID:IMSR_JAX:016830	Transgenic mouse; floxed mice with <i>loxP</i> sites flanking <i>Gabrg2</i>
Genetic reagent (<i>Mus musculus</i>)	Ai9	Jackson Laboratory	JAX Stock# 007909 RRID:IMSR_JAX:00790	Transgenic mouse; cre-dependent tdTomato expression
Genetic reagent (<i>Mus musculus</i>)	<i>Grm6-Cre</i>	Rachel Wong (Hoon <i>et al.</i> , 2015)	N/A	Transgenic mouse; cre-driver line
Antibody	Anti-PKC clone MC5 (mouse monoclonal)	Sigma	Catalog # P5704; RRID:AB_477375	(1:1000)
Antibody	Anti-GABA _A α1 (guinea pig polyclonal)	Fritschy and Mohler, 1995	Generated in Jean-Marc Fritschy's Lab	(1:5000)
Antibody	Anti-GABA _C (rabbit polyclonal)	Enz <i>et al.</i>, 1996	Generated in Heinz Wässle and Joachim Bormann's Lab.	(1:500)
Antibody	Anti-Dsred (rabbit polyclonal)	Clontech		(1:1000)
Antibody	Anti-synaptotagmin2 (mouse monoclonal)	Zebrafish International Resource center	Cat# znp-1; RRID:AB_10013783	(1:1000)
Antibody	Anti-calbindin (rabbit polyclonal)	Swant Inc.	Swant Cat# CB38; RRID:AB_10000340	(1:1000)
Antibody	Anti-GABA _A β2/3, (mouse monoclonal)	MilliporeSigma	Cat# MAB341;	(1:500)
Chemical compound, drug	Ames	Sigma	A1420	
Chemical compound, drug	Alexa 594	Thermofisher	A10442	
Chemical compound, drug	Vectashield	Vector Labs	Cat# H-1000, RRID:AB_2336789	
Chemical compound, drug	GABA _A zine (SR-95531)	Sigma	S106	

Continued on next page

Continued

Reagent type (species) or resource	Designation	Source or reference	Identifiers	Additional information
Chemical compound, drug	GABA	Sigma	A2129	
Chemical compound, drug	TPMPA	Tocris	1040	
Software, algorithm	Symphony	https://github.com/symphony-das		
Software, algorithm	ScanImage	http://scanimage.vidriotechnologies.com/ PMID:12801419	RRID:SCR_014307	
Software, algorithm	MATLAB	http://www.mathworks.com/products/matlab/	RRID:SCR_001622	
Software, algorithm	IGOR Pro	https://www.wavemetrics.com/	RRID:SCR_000325	
Software, algorithm	Amira	https://www.thermofisher.com/global/en/home/industrial/electron-microscopy/electron-microscopy-instruments-workflow-solutions/3d-visualization-analysis-software/amira-life-sciences-biomedical.html	RRID:SCR_007353	
Software, algorithm	ImageJ	https://ImageJ.net	RRID:SCR_003070	

Animal handling and ethic statement

All experiments and animal care were conducted in accordance with the Institutional Animal Care and Use Committee (IACUC) of the University of Wisconsin-Madison and the National Institutes of Health. Animals were housed in a 12 hr light/dark cycle. Ai9/*Grm6Cre*/*Gabrg2* cKO and littermate control adult (2–4 months) mice of both sexes were used in this study. The Ai9/*Grm6Cre*/*Gabrg2* triple transgenic mouse line was chosen because it allowed for selective perturbation of inhibitory receptor GABA_A expression specifically in ON (RBC and T6 CBCs) BCs by genetic deletion of *Gabrg2* (GABA_A receptor, subunit gamma 2) in these cells (Hoon *et al.*, 2015). Loss of *Gabrg2* causes reduced presence of axonal but not dendritic GABA_Aα1 receptors in T6 CBCs (Hoon *et al.*, 2015). The triple transgenic was created by crossing *Gabrg2* floxed mutant mice (Jackson Laboratory, RRID:IMSR_JAX:016830) (Schweizer *et al.*, 2003) with a transgenic mouse line *Grm6*-Cre in which Cre-recombinase is expressed by ON BCs shortly after their differentiation (Hoon *et al.*, 2015; Kerschensteiner *et al.*, 2009; Morgan *et al.*, 2006). In order to label Cre-expressing cells with the red fluorescent protein tdTomato, the *Gabrg2* floxed/*Grm6*-Cre mice were further crossed into the Ai9 reporter line (Jackson Laboratory, RRID:IMSR_JAX:00790).

Immunohistochemical labeling

Retinas were isolated in cold oxygenated mouse artificial cerebrospinal fluid (mACSF, pH 7.4, 119 mM NaCl, 2.5 mM KCl, 2.5 mM CaCl₂, 1.3 mM MgCl₂, 1 mM NaH₂PO₄, 11 mM glucose, and 20 mM HEPES). Retinas were flattened onto filter paper (Millipore, HABP013) and fixed for 15 mins in 4% (wt/vol) paraformaldehyde prepared in mACSF. Retinas were rinsed in phosphate buffer (PBS) and then incubated in a blocking solution (5% donkey serum and 0.5% Triton X-100). The retinas were next incubated with primary antibody over 3 nights at 4°C. Primary antibodies used were anti-PKC (1:1000, mouse, Sigma; RRID:AB_477375), anti-Dsred (rabbit 1:1000, Clontech), anti-synaptotagmin 2 (1:1000, mouse, Znp-1 Zebrafish International Resource center; RRID:AB_10013783), anti-calbindin antibody (rabbit, 1:1000, Swant Inc; RRID:AB_10000340), anti-GABA_Aβ2/3 (mouse, 1:500 Millipore-Sigma) anti-GABA_Aα1 receptor subunit (polyclonal guinea-pig, 1:5000, kindly provided by J.M.

Fritschy), and anti-GABA_{Cp} receptor subunit (1:500, rabbit, kindly provided by R. Enz, H. Wassle, and S. Haverkamp). Retinas were thereafter incubated in secondary antibody solution using anti-isotypic Alexa Fluor (1:1000, Invitrogen) conjugates. Retinas were finally mounted on slides with Vectashield antifade mounting medium (Vector Labs; RRID:AB_2336789).

Electrophysiology

Electrophysiology experiments were performed on whole-mounted retinal preparations made from dark-adapted KO and WT mice. Mice were sacrificed via cervical dislocation and enucleation was subsequently performed. Retinas were isolated in oxygenated (95% O₂/5% CO₂) Ames medium (Sigma-Aldrich) at 32–34°C, mounted flat in a recording chamber and perfused with oxygenated Ames medium at a flow rate of ~8 mL/min during recordings. Retinas were mounted ganglion cell side up (Sinha et al., 2016; Sinha et al., 2020) for recordings. The retinas were embedded in agarose and sliced as previously described (Hoon et al., 2015; Sinha et al., 2020) for RBC recordings. Retinal neurons were visualized for patch-clamp recordings using infrared light (>900 nm). All recordings were obtained from the ventral retina. Voltage-clamp recordings from RBCs and ON α GCs were made with pipettes (~10 M Ω for RBCs and 3–4 M Ω for ON α GCs) filled with an intracellular solution containing (in mM) 105 Cs methanesulfonate, 10 tetraethylammonium chloride, 20 HEPES, 10 EGTA, 2 QX-314, 5 Mg-ATP, 0.5 Tris-GTP (~280 mOsm, pH ~7.2 with KOH). For all voltage-clamp recordings, cells were held at estimated inhibitory and excitatory reversal potentials ~–60 mV and ~0 mV respectively in order to measure excitatory or inhibitory synaptic inputs. Absolute voltages were corrected for liquid junction potentials. For puff recordings of RBCs, GABA was applied with a Picospritzer II (General Valve) connected to a patch pipette with a resistance of ~5–7 M Ω . GABA (200 μ M) was prepared in HEPES-buffered Ames medium with 0.1 mM Alexa 488 hydrazide. Puffing duration (50 ms) and direction were chosen such that the axon terminal of the RBC was completely covered by the puff. For the quantification of GABA-evoked currents, peak amplitude relative to the baseline current before stimulus/drug application was determined and averaged across cells. (1,2,5,6-Tetrahydropyridin-4-yl) methylphosphinic acid (TPMPA, 50 μ M; Tocris, Bristol, United Kingdom) and GABAzine (20 μ M; Tocris, Bristol, United Kingdom) were added to the perfusion solution for RBC recordings as indicated. Alexa 594 dye (100–200 μ M) was added to the intracellular solution for the following image acquisition of the exemplar ON α GC shown in **Figure 2A** using the software ScanImage (RRID:SCR_014307) and analysed using the software ImageJ (RRID:SCR_003070). Light responses were recorded from ON α GCs using whole-cell and cell-attached recordings. LED light sources with peak spectral output at 360 or 405 nm respectively were used to deliver full-field light stimuli that were 500 μ m in diameter and focused on the photoreceptor layer through the optics of the microscope. Photon densities were calibrated using estimations of opsin photoisomerisations per photoreceptor, assuming a rod collecting area of 0.5 μ m² (Field and Rieke, 2002) and a cone collecting area of 0.2 μ m² (Nikonov et al., 2006). Recordings were made in darkness or background light levels at which rods dominate retinal responses and light levels at which cones dominate (~1000 R*/S cone/s).

Electrophysiology data acquisition and analysis

All electrophysiology data was low pass-filtered at 3 kHz, digitized at 10 kHz, and acquired using a Multiclamp 700B amplifier. The data was acquired using Symphony Data Acquisition Software, an open-source, MATLAB-based electrophysiology software (<https://github.com/symphony-das>). Subsequent data analysis was performed using self-written code in MATLAB (Mathworks; RRID:SCR_001622) and Igor Pro (WaveMetrics; RRID:SCR_000325). Peak response amplitudes of ON α GC were quantified by taking the peak spike rate or current during the stimulus presentation. The sustained component of ON α GC response to the 0.5 s light step was estimated by taking the average spike rate or excitatory current over a 200 ms time window (from 0.3 to 0.5 s) from the time of stimulus. The total spike response in **Figure 2C** was estimated as the average spike rate over the duration of the 0.5 s light step. Time to peak was estimated as the time taken for the response to reach from the stimulus onset to the peak amplitude. Decay time was estimated as the time taken for the response to recover from the peak amplitude to a value equal to the pre-stimulus baseline. The time of onset for the sustained phase in **Figure 3—figure supplement 1C–E** was estimated using two approaches – (i) on a per trace basis as the time after the stimulus onset to when the response

reached a fit line with zero slope and (ii) by fitting an exponential function to the response (average traces across trials from each cell) from the end of the transient phase (~175 ms from the time of stimulus onset) to the end of the stimulus and defining the onset time as the time at which the exponential fit decays to 20% of its initial value. Both analysis approaches yielded similar results (**Figure 3—figure supplement 1D,E**). Rebound amplitude for flash responses in **Figure 3M** was estimated as the amplitude of the peak of the overshoot from the baseline.

LN models (**Figure 4**) were derived from ON α GC responses to randomly varying light stimuli (Gaussian distribution of light intensities with standard deviation = 50% of mean intensity; 0–60 Hz bandwidth) as previously described (**Kim and Rieke, 2001; Rieke, 2001; Sinha et al., 2017; Sinha et al., 2016**). The linear temporal filter and the static nonlinearity were estimated using previously described methods (**Kim and Rieke, 2001**). Contrast-dependent changes are shared by the y-axis of the linear filter and the x-axis of the static nonlinearity. Therefore, to estimate the contrast gain unambiguously we needed to scale the linear filter in amplitude such that the variance of the filtered stimulus was equal to the variance of the stimulus. By scaling the filter in this way, differences in the contrast gain of the model would be reflected in changes in the slope of the static nonlinearity. The slope of the static nonlinearity was estimated as the average slope within the linear region of a quintic polynomial fit to each response in KO and WT retina. The slopes estimated from fits with a cumulative density function yielded similar values (data not shown).

Confocal microscopy and image analysis

A Leica SP8 confocal microscope and a 1.4 NA 63 \times oil immersion objective at a voxel size of around 0.05–0.05–0.3 μm (x–y–z) was used to acquire the images in this study. The image stacks acquired were further processed in Amira (Thermo Fisher Scientific; RRID:SCR_007353) software. BC processes were masked in 3D using the *LabelField* function of Amira. Following masking, the receptor signal within the BC process was isolated using the Amira *Arithmetic* tool. A threshold was subsequently applied in order to eliminate background receptor signals and the volume of receptor pixels was expressed as a percent occupancy relative to the volume of the BC processes (for details see **Hoon et al., 2015; Hoon et al., 2017**). A similar procedure was carried out to isolate the GABA $\text{A}\beta$ 2/3 receptor signal within calbindin positive AC and GC processes and ascertain percentage volume occupancy of this receptor signal.

Statistical analysis

We used the unpaired two-tailed t-test for all the statistical analysis. Error bars indicate SEM. The significance threshold was placed at $\alpha = 0.05$ (n.s., $p > 0.05$; * $p < 0.05$; ** $p < 0.01$; *** $p < 0.001$). In all figures, 'n' refers to the number of cells analyzed except in **Figure 1C and D** and **Figure 1—figure supplement 1E** where 'n' refers to number of retinas analyzed.

Acknowledgements

We thank JM Fritschy, R Enz, H Wässle, and S Haverkamp for their generous gifts of GABA receptor antibodies. We thank Rachel Wong and B Luscher for the *Gabrg2* floxed mutant mice. We thank Mike Ahlquist and Austin Butala for their technical support and all members of the lab for their helpful feedback on this project.

Additional information

Funding

Funder	Grant reference number	Author
National Eye Institute	EY026070	Raunak Sinha
University of Wisconsin-Madison	David and Nancy Walsh Family Professorship in Vision Research	Raunak Sinha
University of Wisconsin-Madison	Rebecca Brown Professorship in Vision Research	Mrinalini Hoon

Research to Prevent Blindness		Mrinalini Hoon
National Institute of General Medical Sciences	T32 Graduate Student Fellowship	Jenna Nagy
National Eye Institute	EY031677	Mrinalini Hoon
National Institute of Neurological Disorders and Stroke	T32NS105602	Briana Ebbinghaus

The funders had no role in study design, data collection and interpretation, or the decision to submit the work for publication.

Author contributions

Jenna Nagy, Formal analysis, Writing - original draft, Writing - review and editing, Investigation; Briana Ebbinghaus, Investigation; Mrinalini Hoon, Data curation, Formal analysis, Investigation, Methodology, Writing - original draft, Project administration, Writing - review and editing; Raunak Sinha, Conceptualization, Data curation, Formal analysis, Supervision, Funding acquisition, Investigation, Methodology, Writing - original draft, Writing - review and editing

Author ORCIDs

Raunak Sinha  <https://orcid.org/0000-0002-7553-1274>

Ethics

Animal experimentation: All experiments and animal care were conducted in accordance with the Institutional Animal Care and Use Committee (IACUC) of the University of Wisconsin-Madison and the National Institutes of Health. The protocol was approved by the Animal Care and Use Committee of the University of Wisconsin-Madison (Protocol ID: M006031-R01).

Decision letter and Author response

Decision letter <https://doi.org/10.7554/eLife.60994.sa1>

Author response <https://doi.org/10.7554/eLife.60994.sa2>

Additional files

Supplementary files

- Transparent reporting form

Data availability

All source data shown in the figures including some raw data are available in the data repository, Dryad, accessible via this link <https://doi.org/10.5061/dryad.bg79cnpb4>. Raw datasets are quite large in size and will be made available upon request by the corresponding author.

The following dataset was generated:

Author(s)	Year	Dataset title	Dataset URL	Database and Identifier
Nagy J, Ebbinghaus B, Hoon M, Sinha R	2021	GABAA presynaptic inhibition regulates the gain and kinetics of retinal output neurons	https://doi.org/10.5061/dryad.bg79cnpb4	Dryad Digital Repository, 10.5061/dryad.bg79cnpb4

References

- Asari H, Meister M. 2012. Divergence of visual channels in the inner retina. *Nature Neuroscience* **15**:1581–1589. DOI: <https://doi.org/10.1038/nn.3241>, PMID: 23086336
- Baden T, Berens P, Franke K, Román Rosón M, Bethge M, Euler T. 2016. The functional diversity of retinal ganglion cells in the mouse. *Nature* **529**:345–350. DOI: <https://doi.org/10.1038/nature16468>, PMID: 26735013
- Baden T, Hedwig B. 2010. Primary afferent depolarization and frequency processing in auditory afferents. *Journal of Neuroscience* **30**:14862–14869. DOI: <https://doi.org/10.1523/JNEUROSCI.2734-10.2010>, PMID: 21048145

- Beaudoin DL**, Borghuis BG, Demb JB. 2007. Cellular basis for contrast gain control over the receptive field center of mammalian retinal ganglion cells. *Journal of Neuroscience* **27**:2636–2645. DOI: <https://doi.org/10.1523/JNEUROSCI.4610-06.2007>, PMID: 17344401
- Cangiano L**, Asteriti S, Cervetto L, Gargini C. 2012. The photovoltage of rods and cones in the dark-adapted mouse retina. *The Journal of Physiology* **590**:3841–3855. DOI: <https://doi.org/10.1113/jphysiol.2011.226878>, PMID: 22641773
- Chen C**, Regehr WG. 2003. Presynaptic modulation of the retinogeniculate synapse. *The Journal of Neuroscience* **23**:3130–3135. DOI: <https://doi.org/10.1523/JNEUROSCI.23-08-03130.2003>, PMID: 12716920
- Demb JB**, Singer JH. 2015. Functional circuitry of the retina. *Annual Review of Vision Science* **1**:263–289. DOI: <https://doi.org/10.1146/annurev-vision-082114-035334>, PMID: 28532365
- Diamond JS**, Lukasiewicz PD. 2012. Amacrine cells: seeing the forest and the trees. *Visual Neuroscience* **29**:1–2. DOI: <https://doi.org/10.1017/S0952523812000016>, PMID: 22416288
- Eggers ED**, McCall MA, Lukasiewicz PD. 2007. Presynaptic inhibition differentially shapes transmission in distinct circuits in the mouse retina. *The Journal of Physiology* **582**:569–582. DOI: <https://doi.org/10.1113/jphysiol.2007.131763>, PMID: 17463042
- Eggers ED**, Lukasiewicz PD. 2006. GABA(A), GABA(C) and glycine receptor-mediated inhibition differentially affects light-evoked signalling from mouse retinal rod bipolar cells. *The Journal of Physiology* **572**:215–225. DOI: <https://doi.org/10.1113/jphysiol.2005.103648>, PMID: 16439422
- Eggers ED**, Lukasiewicz PD. 2011. Multiple pathways of inhibition shape bipolar cell responses in the retina. *Visual Neuroscience* **28**:95–108. DOI: <https://doi.org/10.1017/S0952523810000209>, PMID: 20932357
- Enz R**, Brandstätter JH, Wässle H, Bormann J. 1996. Immunocytochemical localization of the GABA_A receptor rho subunits in the mammalian retina. *J Neurosci* **16**:4479–4490.
- Euler T**, Haverkamp S, Schubert T, Baden T. 2014. Retinal bipolar cells: elementary building blocks of vision. *Nature Reviews Neuroscience* **15**:507–519. DOI: <https://doi.org/10.1038/nrn3783>, PMID: 25158357
- Field GD**, Sampath AP, Rieke F. 2005. Retinal processing near absolute threshold: from behavior to mechanism. *Annual Review of Physiology* **67**:491–514. DOI: <https://doi.org/10.1146/annurev.physiol.67.031103.151256>, PMID: 15709967
- Field GD**, Rieke F. 2002. Nonlinear signal transfer from mouse rods to bipolar cells and implications for visual sensitivity. *Neuron* **34**:773–785. DOI: [https://doi.org/10.1016/S0896-6273\(02\)00700-6](https://doi.org/10.1016/S0896-6273(02)00700-6), PMID: 12062023
- Fink AJ**, Croce KR, Huang ZJ, Abbott LF, Jessell TM, Azim E. 2014. Presynaptic inhibition of spinal sensory feedback ensures smooth movement. *Nature* **509**:43–48. DOI: <https://doi.org/10.1038/nature13276>, PMID: 24784215
- Fletcher EL**, Koulen P, Wässle H. 1998. GABA_A and GABA_B receptors on mammalian rod bipolar cells. *The Journal of Comparative Neurology* **396**:351–365. DOI: [https://doi.org/10.1002/\(SICI\)1096-9861\(19980706\)396:3<351::AID-CNE6>3.0.CO;2-1](https://doi.org/10.1002/(SICI)1096-9861(19980706)396:3<351::AID-CNE6>3.0.CO;2-1), PMID: 9624589
- Frerking M**, Ohliger-Frerking P. 2006. Functional consequences of presynaptic inhibition during behaviorally relevant activity. *Journal of Neurophysiology* **96**:2139–2143. DOI: <https://doi.org/10.1152/jn.00243.2006>, PMID: 16775209
- Fritschy J-M**, Mohler H. 1995. GABA_A-receptor heterogeneity in the adult rat brain: differential regional and cellular distribution of seven major subunits. *The Journal of Comparative Neurology* **359**:154–194. DOI: <https://doi.org/10.1002/cne.903590111>
- Greferath U**, Grünert U, Fritschy JM, Stephenson A, Möhler H, Wässle H. 1995. GABA_A receptor subunits have differential distributions in the rat retina: in situ hybridization and immunohistochemistry. *Journal of Comparative Neurology* **353**:553–571. DOI: <https://doi.org/10.1002/cne.903530407>, PMID: 7759615
- Grimes WN**, Zhang J, Graydon CW, Kachar B, Diamond JS. 2010. Retinal parallel processors: more than 100 independent microcircuits operate within a single interneuron. *Neuron* **65**:873–885. DOI: <https://doi.org/10.1016/j.neuron.2010.02.028>, PMID: 20346762
- Grimes WN**, Hoon M, Briggman KL, Wong RO, Rieke F. 2014a. Cross-synaptic synchrony and transmission of signal and noise across the mouse retina. *eLife* **3**:e03892. DOI: <https://doi.org/10.7554/eLife.03892>, PMID: 25180102
- Grimes WN**, Schwartz GW, Rieke F. 2014b. The synaptic and circuit mechanisms underlying a change in spatial encoding in the retina. *Neuron* **82**:460–473. DOI: <https://doi.org/10.1016/j.neuron.2014.02.037>, PMID: 24742466
- Grimes WN**, Zhang J, Tian H, Graydon CW, Hoon M, Rieke F, Diamond JS. 2015. Complex inhibitory microcircuitry regulates retinal signaling near visual threshold. *Journal of Neurophysiology* **114**:341–353. DOI: <https://doi.org/10.1152/jn.00017.2015>, PMID: 25972578
- Grimes WN**, Baudin J, Azevedo AW, Rieke F. 2018. Range, routing and kinetics of rod signaling in primate retina. *eLife* **7**:e38281. DOI: <https://doi.org/10.7554/eLife.38281>, PMID: 30299254
- Haverkamp S**, Wässle H. 2000. Immunocytochemical analysis of the mouse retina. *The Journal of Comparative Neurology* **424**:1–23. DOI: [https://doi.org/10.1002/1096-9861\(20000814\)424:1<1::AID-CNE1>3.0.CO;2-V](https://doi.org/10.1002/1096-9861(20000814)424:1<1::AID-CNE1>3.0.CO;2-V), PMID: 10888735
- Hoon M**, Okawa H, Della Santina L, Wong RO. 2014. Functional architecture of the retina: development and disease. *Progress in Retinal and Eye Research* **42**:44–84. DOI: <https://doi.org/10.1016/j.preteyeres.2014.06.003>, PMID: 24984227
- Hoon M**, Sinha R, Okawa H, Suzuki SC, Hirano AA, Brecha N, Rieke F, Wong RO. 2015. Neurotransmission plays contrasting roles in the maturation of inhibitory synapses on axons and dendrites of retinal bipolar cells. *PNAS* **112**:12840–12845. DOI: <https://doi.org/10.1073/pnas.1510483112>, PMID: 26420868

- Hoon M, Sinha R, Okawa H. 2017. Using fluorescent markers to estimate synaptic connectivity in situ. *Methods in Molecular Biology* **1538**:293–320. DOI: https://doi.org/10.1007/978-1-4939-6688-2_20, PMID: 27943198
- Ingram NT, Sampath AP, Fain GL. 2016. Why are rods more sensitive than cones? *The Journal of Physiology* **594**: 5415–5426. DOI: <https://doi.org/10.1113/JP272556>, PMID: 27218707
- Isaacson JS, Scanziani M. 2011. How inhibition shapes cortical activity. *Neuron* **72**:231–243. DOI: <https://doi.org/10.1016/j.neuron.2011.09.027>, PMID: 22017986
- Jadzinsky PD, Baccus SA. 2013. Transformation of visual signals by inhibitory interneurons in retinal circuits. *Annual Review of Neuroscience* **36**:403–428. DOI: <https://doi.org/10.1146/annurev-neuro-062012-170315>, PMID: 23724996
- Kerschensteiner D, Morgan JL, Parker ED, Lewis RM, Wong RO. 2009. Neurotransmission selectively regulates synapse formation in parallel circuits in vivo. *Nature* **460**:1016–1020. DOI: <https://doi.org/10.1038/nature08236>, PMID: 19693082
- Kim KJ, Rieke F. 2001. Temporal contrast adaptation in the input and output signals of salamander retinal ganglion cells. *The Journal of Neuroscience* **21**:287–299. DOI: <https://doi.org/10.1523/JNEUROSCI.21-01-00287.2001>, PMID: 11150346
- Lukasiewicz PD, Eggers ED, Sagdullaev BT, McCall MA. 2004. GABAC receptor-mediated inhibition in the retina. *Vision Research* **44**:3289–3296. DOI: <https://doi.org/10.1016/j.visres.2004.07.023>, PMID: 15535996
- MacDermott AB, Role LW, Siegelbaum SA. 1999. Presynaptic ionotropic receptors and the control of transmitter release. *Annual Review of Neuroscience* **22**:443–485. DOI: <https://doi.org/10.1146/annurev.neuro.22.1.443>, PMID: 10202545
- Matthews G, Ayoub GS, Heidelberger R. 1994. Presynaptic inhibition by GABA is mediated via two distinct GABA receptors with novel pharmacology. *The Journal of Neuroscience* **14**:1079–1090. DOI: <https://doi.org/10.1523/JNEUROSCI.14-03-01079.1994>, PMID: 7509862
- Morgan JL, Dhingra A, Vardi N, Wong RO. 2006. Axons and dendrites originate from neuroepithelial-like processes of retinal bipolar cells. *Nature Neuroscience* **9**:85–92. DOI: <https://doi.org/10.1038/nn1615>, PMID: 16341211
- Murphy GJ, Rieke F. 2006. Network variability limits stimulus-evoked spike timing precision in retinal ganglion cells. *Neuron* **52**:511–524. DOI: <https://doi.org/10.1016/j.neuron.2006.09.014>, PMID: 17088216
- Neher E, Sakaba T. 2008. Multiple roles of calcium ions in the regulation of neurotransmitter release. *Neuron* **59**: 861–872. DOI: <https://doi.org/10.1016/j.neuron.2008.08.019>, PMID: 18817727
- Nikonov SS, Kholodenko R, Lem J, Pugh EN. 2006. Physiological features of the S- and M-cone photoreceptors of wild-type mice from single-cell recordings. *Journal of General Physiology* **127**:359–374. DOI: <https://doi.org/10.1085/jgp.200609490>, PMID: 16567464
- Oesch NW, Diamond JS. 2011. Ribbon synapses compute temporal contrast and encode luminance in retinal rod bipolar cells. *Nature Neuroscience* **14**:1555–1561. DOI: <https://doi.org/10.1038/nn.2945>, PMID: 22019730
- Oesch NW, Diamond JS. 2019. Synaptic inhibition tunes contrast computation in the retina. *Visual Neuroscience* **36**:E006. DOI: <https://doi.org/10.1017/S095252381900004X>, PMID: 31199207
- Ohliger-Frerking P, Wiebe SP, Stäubli U, Frerking M. 2003. GABA(B) receptor-mediated presynaptic inhibition has history-dependent effects on synaptic transmission during physiologically relevant spike trains. *The Journal of Neuroscience* **23**:4809–4814. DOI: <https://doi.org/10.1523/JNEUROSCI.23-12-04809.2003>, PMID: 12832501
- Olsen SR, Wilson RI. 2008. Lateral presynaptic inhibition mediates gain control in an olfactory circuit. *Nature* **452**: 956–960. DOI: <https://doi.org/10.1038/nature06864>, PMID: 18344978
- Pan F, Toychiev A, Zhang Y, Atlasz T, Ramakrishnan H, Roy K, Völgyi B, Akopian A, Bloomfield SA. 2016. Inhibitory masking controls the threshold sensitivity of retinal ganglion cells. *The Journal of Physiology* **594**: 6679–6699. DOI: <https://doi.org/10.1113/JP272267>, PMID: 27350405
- Raccuglia D, McCurdy LY, Demir M, Gorur-Shandilya S, Kunst M, Emonet T, Nitabach MN. 2016. Presynaptic GABA receptors mediate temporal contrast enhancement in *Drosophila* olfactory sensory neurons and modulate Odor-Driven behavioral kinetics. *Eneuro* **3**:ENEURO.0080-16.2016. DOI: <https://doi.org/10.1523/ENEURO.0080-16.2016>, PMID: 27588305
- Rieke F. 2001. Temporal contrast adaptation in salamander bipolar cells. *The Journal of Neuroscience* **21**:9445–9454. DOI: <https://doi.org/10.1523/JNEUROSCI.21-23-09445.2001>, PMID: 11717378
- Rieke F, Rudd ME. 2009. The challenges natural images pose for visual adaptation. *Neuron* **64**:605–616. DOI: <https://doi.org/10.1016/j.neuron.2009.11.028>, PMID: 20005818
- Root CM, Masuyama K, Green DS, Enell LE, Nässel DR, Lee CH, Wang JW. 2008. A presynaptic gain control mechanism fine-tunes olfactory behavior. *Neuron* **59**:311–321. DOI: <https://doi.org/10.1016/j.neuron.2008.07.003>, PMID: 18667158
- Sagdullaev BT, McCall MA, Lukasiewicz PD. 2006. Presynaptic inhibition modulates spillover, creating distinct dynamic response ranges of sensory output. *Neuron* **50**:923–935. DOI: <https://doi.org/10.1016/j.neuron.2006.05.015>, PMID: 16772173
- Sawant A, Ebbinghaus BN, Bleckert A, Gamlin C, Yu WQ, Berson D, Rudolph U, Sinha R, Hoon M. 2021. Organization and emergence of a mixed GABA-glycine retinal circuit that provides inhibition to mouse ON-sustained alpha retinal ganglion cells. *Cell Reports* **34**:108858. DOI: <https://doi.org/10.1016/j.celrep.2021.108858>, PMID: 33730586
- Schmidt TM, Alam NM, Chen S, Kofuji P, Li W, Prusky GT, Hattar S. 2014. A role for melanopsin in alpha retinal ganglion cells and contrast detection. *Neuron* **82**:781–788. DOI: <https://doi.org/10.1016/j.neuron.2014.03.022>, PMID: 24853938

- Schwartz GW**, Okawa H, Dunn FA, Morgan JL, Kerschensteiner D, Wong RO, Rieke F. 2012. The spatial structure of a nonlinear receptive field. *Nature Neuroscience* **15**:1572–1580. DOI: <https://doi.org/10.1038/nn.3225>, PMID: 23001060
- Schweizer C**, Balsiger S, Bluethmann H, Mansuy IM, Fritschy JM, Mohler H, Lüscher B. 2003. The gamma 2 subunit of GABA(A) receptors is required for maintenance of receptors at mature synapses. *Molecular and Cellular Neuroscience* **24**:442–450. DOI: [https://doi.org/10.1016/S1044-7431\(03\)00202-1](https://doi.org/10.1016/S1044-7431(03)00202-1), PMID: 14572465
- Sinha R**, Lee A, Rieke F, Haeseleer F. 2016. Lack of CaBP1/Caldendrin or CaBP2 leads to altered ganglion cell responses. *Eneuro* **3**:ENEURO.0099-16.2016. DOI: <https://doi.org/10.1523/ENEURO.0099-16.2016>, PMID: 27822497
- Sinha R**, Hoon M, Baudin J, Okawa H, Wong ROL, Rieke F. 2017. Cellular and circuit mechanisms shaping the perceptual properties of the primate fovea. *Cell* **168**:413–426. DOI: <https://doi.org/10.1016/j.cell.2017.01.005>
- Sinha R**, Siddiqui TJ, Padmanabhan N, Wallin J, Zhang C, Karimi B, Rieke F, Craig AM, Wong RO, Hoon M. 2020. LRRTM4: a novel regulator of presynaptic inhibition and ribbon synapse arrangements of retinal bipolar cells. *Neuron* **105**:1007–1017. DOI: <https://doi.org/10.1016/j.neuron.2019.12.028>, PMID: 31974009
- Smeds L**, Takeshita D, Turunen T, Tiihonen J, Westö J, Martyniuk N, Seppänen A, Ala-Laurila P. 2019. Paradoxical rules of spike train decoding revealed at the sensitivity limit of vision. *Neuron* **104**:576–587. DOI: <https://doi.org/10.1016/j.neuron.2019.08.005>
- Sonoda T**, Lee SK, Birnbaumer L, Schmidt TM. 2018. Melanopsin Phototransduction Is Repurposed by ipRGC Subtypes to Shape the Function of Distinct Visual Circuits. *Neuron* **99**:754–767. DOI: <https://doi.org/10.1016/j.neuron.2018.06.032>, PMID: 30017393
- van Wyk M**, Wässle H, Taylor WR. 2009. Receptive field properties of ON- and OFF-ganglion cells in the mouse retina. *Visual Neuroscience* **26**:297–308. DOI: <https://doi.org/10.1017/S0952523809990137>, PMID: 19602302
- Völgyi B**, Xin D, Bloomfield SA. 2002. Feedback inhibition in the inner plexiform layer underlies the surround-mediated responses of All amacrine cells in the mammalian retina. *The Journal of Physiology* **539**:603–614. DOI: <https://doi.org/10.1113/jphysiol.2001.013133>, PMID: 11882691
- Wässle H**, Koulen P, Brandstätter JH, Fletcher EL, Becker CM. 1998. Glycine and GABA receptors in the mammalian retina. *Vision Research* **38**:1411–1430. DOI: [https://doi.org/10.1016/S0042-6989\(97\)00300-3](https://doi.org/10.1016/S0042-6989(97)00300-3), PMID: 9667008